

Tunable photonic devices based on the temperature dependent photonic band gap in chiral nematic liquid crystals

Yuhua Huang, Ying Zhou, and Shin-Tson Wu

College of Optics and Photonics, University of Central Florida, Orlando, Florida 32816

ABSTRACT

We have investigated the physical and optical properties of the left-handed chiral dopant ZLI-811 mixed in a nematic liquid crystal (LC) host BL006. The solubility of ZLI-811 in BL006 at room temperature is ~24 wt%, but can be enhanced by increasing the temperature. Consequently, the photonic band gap of the cholesteric liquid crystal (CLC) mixed with more than 24 wt% chiral dopant ZLI-811 is blue shifted as the temperature increases. Based on this property, we demonstrate its applications in thermally tunable band-pass filters and dye-doped CLC lasers. In addition, we also demonstrated a spatially tunable laser emission by generating a one-dimensional temperature gradient along the dye-doped cholesteric liquid crystal (CLC) cell. The lasing wavelength is widely tunable from 577 nm to 670 nm. The lowest excitation energy and maximum lasing efficiency occur at $\lambda \sim 605$ nm which corresponds to the peak fluorescence emission of the dye.

1. INTRODUCTION

Cholesteric liquid crystal (CLC) is a simple one-dimensional photonic crystal and has many interesting applications because of their unique properties and simple fabrication process [1-4]. A CLC is formed by rod-like molecules whose directors are self-organized in a helical structure. In the planes perpendicular to the helical axis, the LC directors are continuously rotated along the helical axis. By choosing a high birefringence LC, the periodic helical structure gives rise to a periodic modulation of the refractive index, which results in a selective reflection band. Within the band, the circularly polarized incident light with the same handedness as the cholesteric helix is reflected while the opposite handedness is transmitted. The frequency range of the reflection band is determined by the ordinary (n_o) and extraordinary (n_e) refractive indices of the LC, and the pitch length (p) of the helical structure. The reflection band edges occur at $\lambda_1 = n_o p$ and $\lambda_2 = n_e p$, where p is the helical pitch length.

A CLC cell is typically prepared by doping some chiral agents into a nematic liquid crystal mixture. The fabrication process is quite simple. Moreover, the electromagnetic characteristics of CLC photonic band gap (PBG) can be easily controlled by adjusting the LC or chiral parameters, or by adjusting the external factors such as temperature, pressure, light irradiation, or electric field [4-10]. For example, the CLC PBG can be switched on and off by an electric field, which can be used as a bistable light shutter [8]. The frequency range of the PBG can be varied by irradiating the CLC sample with a UV light, which has been demonstrated for tunable laser applications [7, 8]. In addition, temperature has also been widely used to modify the CLC PBG's frequency range [9-11]. In most cases, the modification of the CLC PBG's frequency by temperature is based on the dependency of the LC's phase transition or the temperature-dependent birefringence [10, 11].

In this paper, we demonstrate a thermally tunable CLC PBG based on the temperature dependent solubility of the chiral dopant. As the temperature increases, the dopant's solubility increases which, in turn, shortens the pitch length and leads to a blue shift in the reflected spectrum. Based on this property, thermally tunable band-pass filters and dye-doped CLC lasers are demonstrated. Different from prior approaches, our method is mainly based on the temperature dependent chiral solubility in the LC host, rather than the temperature dependent refractive index change [11, 12]. We find that our method is ~600X more sensitive.

2. SAMPLE PREPARATION

In experiment, several different CLC mixtures were prepared by doping a left-handed chiral agent ZLI-811 into BL006 and ZLI-4608 (both are Merck mixtures). The dopant concentration varies from 22 to 36 wt% by 2% interval. The refractive indices for BL006 are $n_e=1.816$ and $n_o=1.530$ and for ZLI-4608 are $n_e=1.656$ and $n_o=1.499$ at $T=20$ °C and $\lambda=589$ nm. The mixtures were stirred in isotropic phase at ~ 120 °C for ~ 4 h to make the constituents uniformly mixed and then capillary filled into a 10 μm gap LC cell in the isotropic phase. The inner surfaces of the glass substrates were coated with a thin polyimide alignment layer and rubbed in anti-parallel directions. The pretilt angle is $\sim 3^\circ$. After the temperature was gradually cooled down to room temperature, a CLC sample with left-handed (LH) helix was formed.

3. RESULTS AND DISCUSSION

First, we compared the optical properties of the CLC samples prepared in the BL006 host versus those in the LC ZLI-4608 host. The transmission spectra of the CLC samples were measured using a spectrophotometer. Here, we just take two CLC mixtures with 22 wt% ZLI-811 in BL006 and ZLI-4608 as examples to illustrate the host LC effect on the PBG. Results are plotted in Fig. 1. Although the two CLC samples contain the same concentration of ZLI-811, their PBGs occur at different spectral range and their bandwidth is also different because of the different refractive indices and birefringence of the LC hosts. Since ZLI-4608 has a smaller n_o and Δn than BL006, under the same chiral concentration, its CLC PBG occurs at a shorter wavelength and its bandwidth is narrower. According to the PBG transmission spectrum, we can calculate the helical pitch length (P) and the helix twist power (HTP) of ZLI-811 in the two different LC hosts using the following equations [13]:

$$P = \lambda_o / n , \quad (1)$$

$$HTP = 1/(C \times P) , \quad (2)$$

where λ_o is the central wavelength of the photonic bandgap, $n = (n_e + n_o) / 2$ is the average refractive index, and C is the chiral concentration. The pitch length and helix twist power of ZLI-811 are calculated to be [404.47 nm, $10.30 \mu\text{m}^{-1}$] and [394.39 nm, $10.56 \mu\text{m}^{-1}$] for the BL006 and ZLI-4608 hosts, respectively.

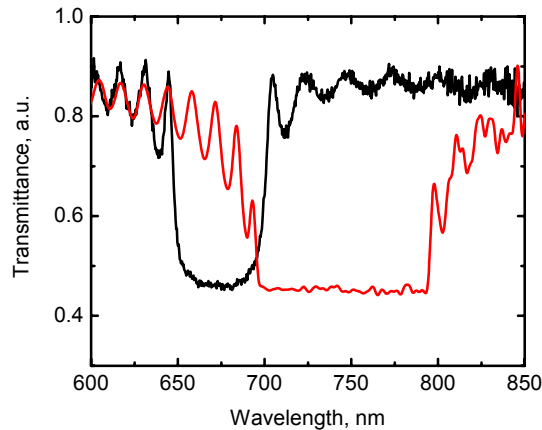


Fig. 1: The transmission spectra of the CLC cells mixed with 22 wt% ZLI-811 in BL006 (red line) and ZLI-4608 (black line) hosts, respectively.

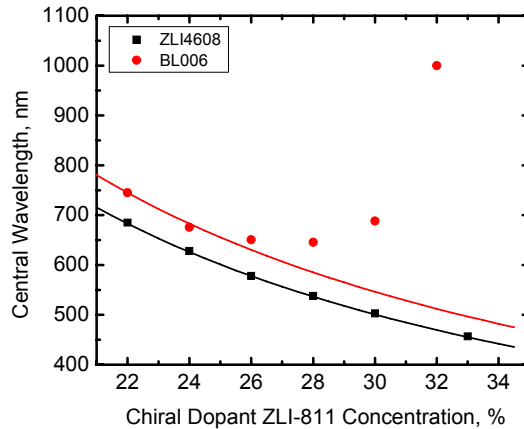


Fig. 2: Experimental and simulated results of the central wavelength of the CLC PBG with respect to the chiral dopant concentration in two different LC hosts: BL006 and ZLI-4608.

From the PBG transmission spectrum, we extracted the central wavelength by averaging the wavelength of the PBG at the short and long edges. Figure 2 shows the dependence of the central wavelength of the PBG on the chiral dopant concentration. The symbols are the experimental results and the solid lines are the simulation results based on the following relationship:

$$\lambda_o = nP = \frac{n}{HTP \times C} \quad (3)$$

From Fig. 2, the experimental results agree with theory quite well for the ZLI-4608 host. As the dopant concentration increases, the central reflection wavelength decreases according to Eq. (3). However, a big discrepancy occurs for the BL006 samples as the dopant concentration exceeds 24 wt%. To understand this discrepancy, we studied the temperature effect on the PBG of the BL006-based CLC samples with more than 24 wt% chiral ZLI-811.

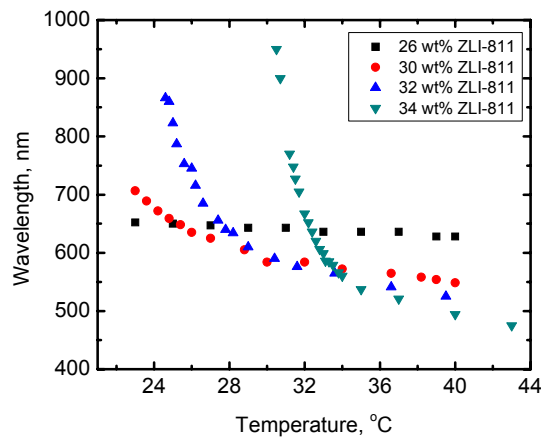


Fig. 3: Temperature dependent central wavelength of the CLC PBG.

Figure 3 shows the temperature dependent PBG's central wavelength for the BL006- based CLC samples with 26, 30, 32, and 34 wt% of chiral ZLI-811. For the well dissolved CLC sample with less than 24% chiral dopant, increasing the temperature will reduce the band gap and shrink the band edge towards the central wavelength due to the refractive index change, but barely shift the central wavelength. From Fig.3, we can see that as the temperature increases, the central wavelength of the CLCs' PBG is obviously blue

shifted. The blue shift of a CLC with a lower chiral dopant concentration saturates at a lower temperature and, moreover, its final PBG appears at a longer wavelength than those with a higher chiral concentration. When the blue shift of the PBG is stopped, the central wavelength of the PBG follows the chiral concentration according to Eq. (3). This indicates that at room temperature, 26 wt% of ZLI-811 is already beyond its maximum solubility in BL006. Further increasing the chiral concentration would make a portion of ZLI-811 molecules to precipitate from the BL006 host and aggregate. The aggregation might attract some chiral molecules from the LC host which, in turn, results in a lower effective chiral concentration and consequently a red shift. As a result, the PBG shifts toward a longer wavelength, as shown in Fig. 2. Since a higher temperature enhances the solubility of the chiral dopant in the LC which shortens the pitch length of the CLC's helix, the PBG of CLCs produces blue shift as the temperature increases. A higher concentration of ZLI-811 needs a higher temperature to be totally dissolved in the BL006 LC host.

To show the phase separation and aggregation of ZLI-811 from BL006, we took the images of the CLC samples under a polarizing optical microscope. Figure 4(a) shows the microscopic photos of the CLCs doped with different chiral concentration in BL006 at room temperature ($T \sim 23^\circ\text{C}$). It is difficult to see the phase separation when the chiral concentration is below 30 wt%. However, when the chiral concentration is above 32 wt%, the phase separation is quite distinct. For example, the 34 wt% ZLI-811 CLC sample no longer exhibits a planar cholesteric structure; instead, most part of the sample is enclosed by chain-like structures. The sample is not transparent but scatters light. The chain-like structures are induced by the phase separation and aggregation of the chiral molecules from BL006. As the temperature is increased to $\sim 26.5^\circ\text{C}$, the sample starts to become transparent again because more chiral molecules are dissolved in BL006. Further increasing the temperature makes the sample more and more transparent and the planar helical structure more uniform, as Fig. 4(b) shows.

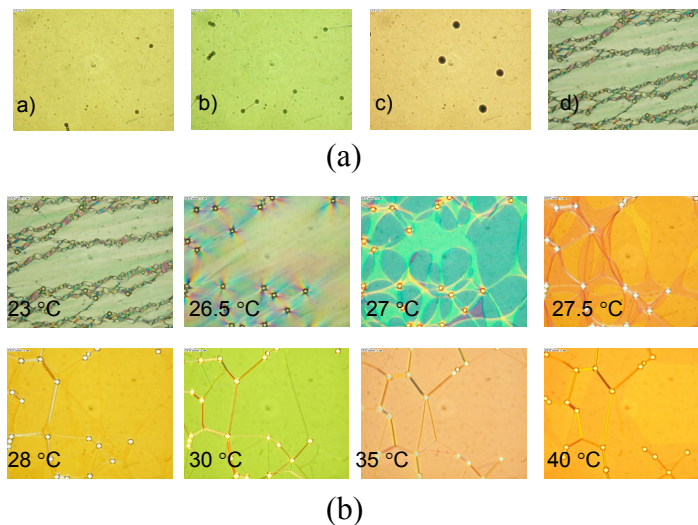


Fig. 4: (a) The microscope photos of the CLCs with different chiral dopant ZLI-811 concentrations: a) 24 wt%, b) 28 wt%, c) 32 wt%, and d) 34 wt%; (b) the microscope photos of the CLCs with 34 wt% chiral dopant ZLI-811 at different temperature.

4. PHOTONIC APPLICATIONS

This temperature dependent CLC PBG property can be used for tuning the band pass of a filter. Here, we take the CLC sample with 34 wt% chiral dopant ZLI-811 in the BL006 host as an example to demonstrate the potential applications. Results are illustrated in Fig. 5. Figure 5 shows the reflected color of the CLC captured by a digital camera at different temperatures. The reflected color of the CLC sample changes from red to blue as the temperature is increased from 30°C to 50°C . Since this CLC sample has left-handed helix, it is only useful for left circular polarization. We can obtain polarization independent bandpass filter by stacking two CLC samples with left- and right-handed helices.

The most attractive application of the temperature dependent CLC PBG property is for tunable laser applications by doping some laser dyes into the CLC mixture. To demonstrate the thermally tunable laser application, we added 1 wt% of laser dye 4-(dicyanomethylene)- 2-methyl-6-(4-dimethylaminostryl)-4H-pyran (DCM, Exciton) into the CLC mixture with 34 wt% chiral dopant ZLI-811 and then injected the well mixed dye doped CLC mixtures into an 8 μm LC cell. Figure 6 shows the normalized laser emission spectra from the dye doped CLC sample under the excitation of $\sim 16\mu\text{J}$ pulse energy from a second-harmonic Nd:YAG laser at $\lambda=532$ nm with 4 ns pulse width and 1 Hz repetition rate. The lasing wavelength with ~ 1 nm line width can be tuned from 645 nm to 580 nm by merely changing the sample temperature from 26.2 $^{\circ}\text{C}$ to 28.7 $^{\circ}\text{C}$. The lasing intensity strongly depends on the lasing wavelength, as can be seen in Fig. 4. The highest lasing intensity is obtained at ~ 605 nm. For the lasing wavelengths away from 605 nm, the lasing intensity was lower. The reason has been explained in detail in Ref [14]. We do not want to repeat it here.



Fig. 5: Temperature dependent CLC bandpass filters.

The temperature dependent lasing wavelengths in Fig.6 seem inconsistent with the temperature dependent PBG of the CLC without dye as shown in Fig.3. We have to point out that the dye used in this experiment enhances the solubility of the chiral in the mixture. From Fig.6, we can see that as the temperature is increased, the lasing wavelength is shifted towards short wavelength due to the increased dissolved chiral concentration. However, when the temperature is above a certain value, the slope of the shifted wavelength range over the temperature is decreased with the increased temperature, as seen in Fig. 3 and Fig. 6. The reason is that when the temperature is increased to a certain value, most of the chiral molecules are dissolved in the LC mixture and very few chiral molecules are spared for the further increased temperature. The average change of the CLC PBG's central wavelength reaches 26 nm/ $^{\circ}\text{C}$. In comparison, if we tune the CLC PBG using the temperature dependent refractive index, the calculated change is only 0.05 nm/ $^{\circ}\text{C}$ [12]. Our method is $\sim 600\text{X}$ more sensitive.

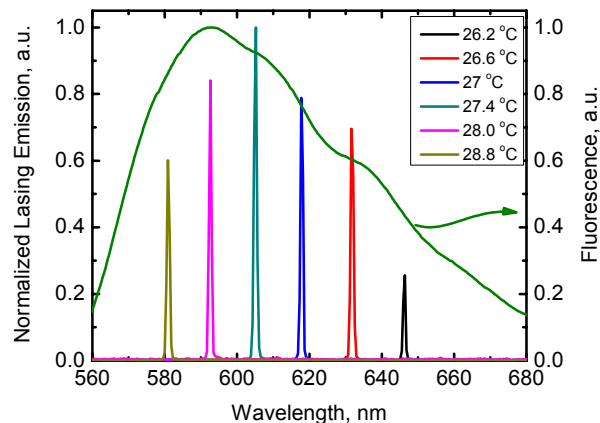


Fig. 6: Temperature dependent (normalized) laser emission wavelength. The CLC sample consists of 34 wt% ZLI-811 in BL-006 host, plus 1 wt% DCM dye. The pumping laser wavelength is $\lambda=532$ nm.

Based on the temperature dependent optical properties of the CLC sample, we can easily obtain a spatially tunable CLC PBG by generating 1D temperature gradient across the CLC cell. To achieve this goal, we simply placed one side of the CLC cell on a heating stage and left the other side in the air. By raising the temperature of the heating stage over room temperature, a 1D temperature gradient was formed. Figure 7 shows the image of a CLC cell with gradient temperature at $T \sim 50^\circ\text{C}$. The reflected colors spread from blue to red as the position gets farther away from the heat source.

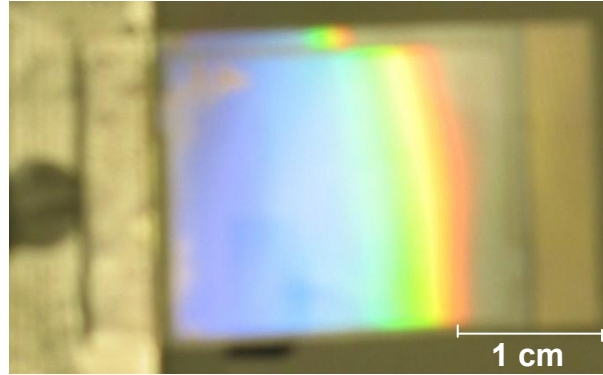


Fig. 7: Image of the gradient CLC reflection band.

By doping some laser dye DCM in it, we can get spatially tunable laser emission under the excitation of the green pump laser. Figure 8 illustrates the normalized laser emission of the dye-doped CLC cells at different positions, i.e., different temperatures. For instance, positions 1-5 correspond to $T \sim 30.6, 28.8, 27.6, 26.8,$ and 26°C , respectively.

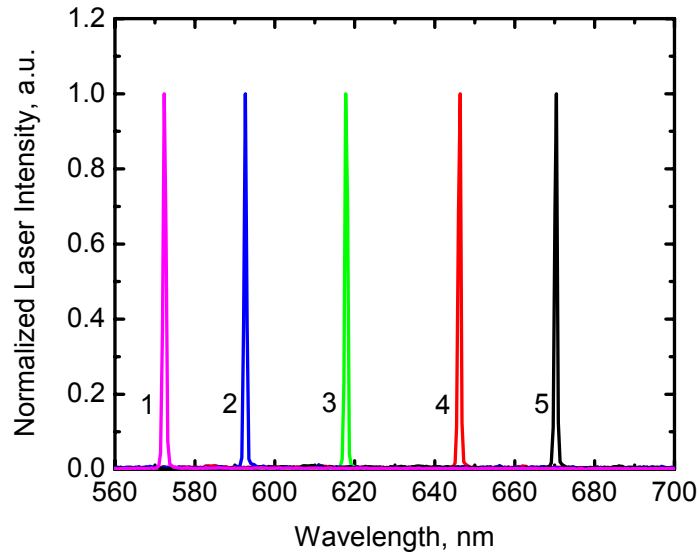


Fig. 8: Normalized laser emission of the dye-doped CLC cells with various PBGs at different sample positions. Positions 1-5 correspond to $T \sim 30.6, 28.8, 27.6, 26.8,$ and 26.0°C , respectively.

In addition, we also investigated the dependence of the lasing emission intensity at different wavelengths on the excitation energy. Figure 4 shows the results we obtained from the dye-doped CLC cell with a PBG at different spectral position by adjusting the position of the dye-doped CLC with respect to the pump beam. For any lasing wavelengths, the emission intensity is significantly enhanced as the excitation energy exceeds the threshold. However, the threshold excitation energy and lasing efficiency strongly depend on the lasing wavelength, as Fig. 4 shows. When the lasing wavelength is at $\lambda = 605\text{ nm}$, the lasing efficiency

reaches the maximum ($\sim 0.5\%$) and threshold excitation energy is the lowest ($\sim 4.7 \mu\text{J}/\text{pulse}$). If the lasing wavelength is away from 605 nm, higher threshold excitation energy is required and the lasing efficiency is decreased. We know that laser emission can be obtained only when the optical gain overcomes the losses in the medium and larger optical gain makes the generation of the laser emission easier because the optical emission is more effectively obtained by the feedback effect. As stated above, the optical gain spectrum relies on the fluorescence spectrum of the dye. Since the DCM dye exhibits its maximum fluorescence at $\lambda \sim 605 \text{ nm}$, the lowest threshold excitation energy of $\sim 4.7 \mu\text{J}/\text{pulse}$ and the highest lasing efficiency occurs for the dye-doped CLC sample when the long edge of the PBG is at 605 nm. When the long edge of the CLC PBG overlaps with the tail of the fluorescence band, higher threshold energy is required for exciting more optical emission to overcome the loss and finally generating the laser feedback effect. Consequently, the lasing efficiency is decreased.

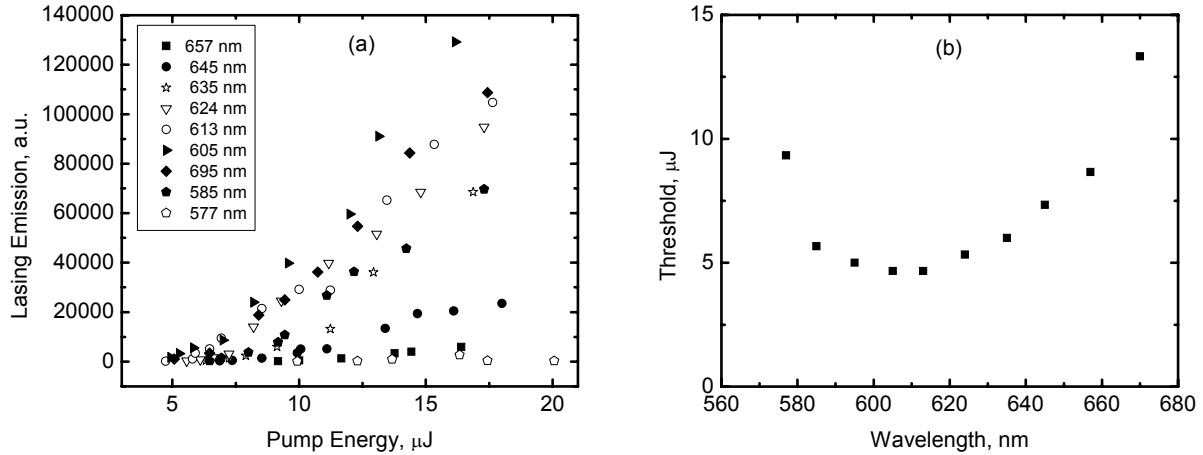


Fig. 7: The laser emission intensity from the dye-doped CLC cell as a function of: (a) the excitation energy of the pumping beam at 532 nm and (b) the threshold excitation energy as a function of the lasing wavelength.

5. Conclusion

We have investigated the physical and optical properties of the chiral agent ZLI-811 doped in the BL006 LC host. The solubility of ZLI-811 in BL006 is limited to 24 wt%. Excessive dopant would result in precipitation and aggregation which leads to light scattering. However, the solubility of ZLI-811 in BL006 can be enhanced by raising the temperature. Since a higher chiral dopant concentration can reduce the pitch length of the helix, the photonic band gap of the cholesteric liquid crystal mixed with more than 24 wt% chiral dopant ZLI-811 is blue shifted with the increase of the temperature. Compared to the thermally tunable CLC PBG based on the temperature dependent refractive index change, our method is $\sim 600\text{X}$ more sensitive. Based on the thermal effect of the CLC, we have demonstrated its applications in thermally and spatially tunable band pass filters and mirrorless lasers.